Defective NETs Clearance contributes to sustained FXII Activation in COVID-19-associated Pulmonary Thrombo-Inflammation

Hanna Englert[1§], Chandini Rangaswamy[1§], Carsten Deppermann[1§], Jan-Peter Sperhake[2], Christoph Krisp[1], Danny Schreier[1], Emma Gordon[3], Sandra Konrath[1], Munif Haddad[1], Giordano Pula[1], Reiner K. Mailer[1], Hartmut Schlüter[1], Florian Langer[4], Klaus Püschel[2], Kosta Panousis[5], Evi X. Stavrou[6], Coen Maas[7], Thomas Renné[1], Maike Frye[1*]

[1]Institute of Clinical Chemistry and Laboratory Medicine, University Medical Center Hamburg-Eppendorf, Hamburg, Germany
[2]Department of Legal Medicine, University Medical Center Hamburg-Eppendorf, Hamburg, Germany
[3]Division of Cell and Developmental Biology, Institute for Molecular Bioscience, The University of Queensland, Brisbane, QLD, Australia
[4] II. Medical Clinic and Polyclinic, University Medical Center Hamburg-Eppendorf, Hamburg, Germany
[5]CSL Limited, BIO21 Institute, Parkville, Victoria, Australia
[6]Department of Medicine, Case Western Reserve University School of Medicine, Cleveland, Ohio, United States
[7]Department of Clinical Chemistry and Haematology, University Medical Center Utrecht, Utrecht, University, Utrecht, the Netherlands

[§]Authors contributed equally.

[*]Corresponding author: Dr. Maike Frye, Institute of Clinical Chemistry and Laboratory Medicine, University Medical Center Hamburg, Martinistr. 52, 20246 Hamburg, Germany, m.frye@uke.de, +49 40 4710 57004

Running title: NETs and FXII in COVID-19
Word count: 4689
Figures: 4

Keywords: COVID-19, thrombosis, FXII, NETs, pulmonary thrombo-inflammation

Abstract

Coagulopathy and inflammation are hallmarks of Coronavirus disease 2019 (COVID-19) and are associated with increased mortality. The mechanisms that drive thrombo-inflammation in COVID-19 are poorly understood. Here, we report a role of the NETs/ Factor XII (FXII) axis for initiating procoagulant and proinflammatory reactions in COVID-19.

Proteomic analysis revealed enrichment of FXII in postmortem lung tissue from COVID-19 patients. Immunofluorescence analysis of COVID-19 lung tissue showed that FXII is activated in the lung parenchyma, within the pulmonary vessel walls and in fibrin-rich alveolar spaces. In particular, activated FXII (FXIIa) colocalized with NETs in COVID-19 lung tissue, indicating that NETs accumulation leads to FXII contact activation in COVID-19. We further showed that an accumulation of NETs is partially caused by impaired NETs clearance via extracellular DNases. In contrast, addition of DNase I improved NETs clearance and reduced FXII activation *in vitro*. We propose that targeting both, FXIIa and the FXII activator NETs, is therapeutically effective in mitigating thrombo-inflammation in COVID-19.

Introduction

The Coronavirus disease 2019 (COVID-19), which has caused over 1.1 million deaths and has infected 40 million people, continues to be a major health care emergency. Although initially considered a respiratory disease, it has now become apparent that during infection with severe acute respiratory syndrome coronavirus type 2 (SARS-CoV-2), a constellation of thrombotic complications occurs. Increased cytokine levels (IL-6, IL-10, and TNF-α) and lymphopenia are reported in severe cases suggesting a cytokine storm as one of the hallmarks of COVID-19 [1,2]. Incidence of thromboembolic events such as deep vein thrombosis (DVT) and systemic thrombotic occlusions in the lung, liver, kidney, brain and heart is high in COVID-19 patients [3-5].

The vascular hyperinflammatory reaction in SARS-CoV-2 infection promotes a prothrombotic state by the activation of various cell types including endothelial cells, platelets, and cells of the innate immune system. In particular, heavy neutrophil infiltration has been reported in the pulmonary interstitial and alveolar spaces in autopsies of COVID-19 patients [6,7]. Neutrophils are essential in the rapid innate immune response to injury [8,9]. Upon activation, neutrophils release neutrophil extracellular traps (NETs), that promote procoagulant reactions involving platelet activation [10] and fibrin generation [11,12]. Factor XII (FXII) is the zymogen of the serine protease FXIIa that initiates the procoagulant and proinflammatory contact system and thereby triggers the intrinsic pathway of coagulation and the bradykinin-forming kallikrein kinin system, respectively (reviewed [13]. NETs bind FXII zymogen [12] and induce coagulation in plasma samples in a FXII-dependent manner [14]. NETs are cleared from tissues and the circulation by endogenous deoxyribonucleases (DNases). We previously showed that defective DNase activity augments NETs-mediated occlusive clot formation and organ damage in non-viral systemic inflammation sepsis models [15,16]. Recent studies revealed elevated NETs biomarkers in serum from COVID-19 patients [17,18]. Furthermore, the accumulation of NETs was demonstrated in fixed lung tissue, as well as in tracheal aspirates of COVID-19 patients on mechanical ventilation [19]. Taken together, there is accumulating evidence that NETs and coagulation play an important role in the pathogenesis of COVID-19.

In the present study, we show that crosstalk of innate immune cells with FXII and the contact system contributes to adverse thrombo-inflammatory reactions in COVID-19 and interference with the NETs/FXII axis offers novel therapeutic strategies for coping with thrombo-inflammation in COVID-19. We screened postmortem lung tissue from three COVID-19 patients using a systemic proteomics approach. Systems biology found FXII enriched in COVID-19 infected lungs, as well as pathways involved in complement activation, platelet activation and neutrophil degranulation. We showed that NETs colocalize with the active serine

protease, FXIIa, in COVID-19 lung tissue indicating that NETs provide a platform for FXII contact activation in COVID-19. Ultimately, we found that NETs degradation by DNases is impaired in plasma from COVID-19 patients, providing a rationale for sustained NETs-induced FXII activity in COVID-19. Taken together, the NETs-FXII axis occupies a central position in COVID-19 and offers novel therapeutic strategies for interference with virus-associated pulmonary thrombo-inflammation.

Methods

Acquisition of patient plasma samples. Heparinized plasma samples were obtained from SARS-CoV-2 positive patients hospitalized at the University Medical Center Hamburg, Germany during the first outbreak in April 2020 (permit number #2322, Ethics Committee of the Hamburg Medical Association, Hamburg, Germany). The inclusion criterion was positive identification of a SARS-CoV-2 infection via PCR analysis.

Quantification of DNase activity in plasma. DNase activity was determined using the DNase Alert QC System (Thermo Fisher Scientific). Substrate solution and 10X nuclease buffer, both provided in the kit, were dispensed into a black 96-well plate. Heparinized plasma was diluted 20-fold in nuclease-free water and added to the respective wells. Fluorescence was measured at excitation/emission maxima of 530/580 nm in a microplate fluorometer (Tecan Spark 10M).

Detection of DNase activity by single radial enzyme diffusion (SRED) assay. DNase activity was measured as previously described [20]. In brief, plasma from COVID-19 patients was loaded into wells of an agarose gel that contained DNA from salmon testes (D1626, Sigma) and SYBR Safe (S33102, Invitrogen). After incubating the gels at 37°C in a humid chamber, DNA fluorescence was recorded with a fluorescence scanner (Biorad). The diameter of DNase digestion was measured using Image J.

NET degradation assay. Purified human neutrophils from healthy volunteers ($5x10^4$ per well) were seeded in serum-free Dulbecco's Modified Eagle's Medium (DMEM, Life Technologies) onto 96-well microplates. Neutrophils were activated with 100 nM phorbol 12-myristate 13-acetate (PMA, Sigma Aldrich) for 4h at 37°C, with 5% CO_2 and humidity between 85-95%. On completion of incubation with PMA, DMEM was aspirated and neutrophils were stored overnight in PBS at 4°C. The following day, serial dilutions of Pulmozyme (500 µg/ml - 7.8 µg/ml) and 10-fold diluted plasma [in HBSS (Life Technologies) with divalent cations] were added to each well and co-incubated with formed NETs for 3h at 37°C with 5% CO_2 and humidity between 85-95%. Plasma was subsequently removed from the plates and fixed with 2% PFA in PBS for 1h. Plates were washed with PBS before they were stained with 2mM of

cell-impermeable DNA dye, Sytox Green (Life Technologies). Fluorescence was quantified using a microplate fluorometer (Tecan Spark 10M); fluorescent images of nuclei and NETs were obtained with an inverted fluorescence microscope (Zeiss Axiovert 200M).

Measurement of FXIIa generation (chromogenic assay). Purified human neutrophils from healthy volunteers were seeded in serum-free DMEM onto sterile 96-well plates at a concentration of $10x10^5$ cells per well. NET formation was induced with 10nM phorbol 12-myristate 13-acetate (PMA; Sigma) for 4h at 37°C, 5 % CO_2 and humidity between 85-95%. Purified human zymogen FXII (30µg/ml, HTI, HCXII-0155) was incubated with neutrophils that were pre-treated with vehicle or DNase I (10U/ml, Dornase alpha, Roche, Germany) for 1h, in the absence or presence of the FXIIa inhibitor, hHA-infestin-4 (500µg/ml, CSL Behring). The enzymatic activity of FXIIa was measured photometrically using the chromogenic substrate S-2302 (1mM, Chromogenix) at an absorbance wavelength of 405nm.

Autopsies. The COVID19 autopsy cases were part of a larger consecutive case series [5]. The deceased patients were PCR-positive for SARS-CoV-2 in throat or lung swabs and had both deep vein thrombosis of the lower extremities and pulmonary embolism at the time of death. For control, tissue samples were used from non-COVID19 infected patients who expired in the intensive care unit of the University Medical Center, Hamburg-Eppendorf. Access to these postmortem tissues was granted by the Ethics Committee of the Hamburg Medical Association with a positive opinion on the examination of the tissue obtained postmortem (reference number PV7311).

Immunofluorescence staining of human lung tissue. For visualization of lung tissue, 300 µm vibratome cross sections of formalin-fixed control or COVID-19 lung tissue were used for staining. Sections were permeabilized using 0.5% Triton-X100 in PBS for 20min at RT followed by blocking with 3% BSA in PBSTx for 2h. Primary antibodies were incubated overnight at 4°C, washed three times with PBSTx and subsequently incubated with secondary antibodies overnight at 4°C before further washing and mounting in Dako fluorescence mounting medium. The following antibodies were used: anti-neutrophil elastase (5 µg/ml, ab121595, Abcam), anti-chromatin (anti-histone H2A/H2B/DNA-complex, 5 µg/ml, Davids Biotechnologie GmbH [21]), anti-Collagen I (5 µg/ml, Ab34710, Abcam), anti-fibrin (5 µg/ml, MABS2155, Merck), AlexaFluor488-conjugated anti-FXIIa (10 µg/ml, 3F7, CSL Limited), anti-citrullinated histone H3 (1:500, ab5103, Abcam). Secondary antibodies conjugated to AlexaFluor-488, -594 and -647 were obtained from Jackson ImmunoResearch (all donkey, used in 1:200 dilution). Confocal tissue images represent maximum intensity projections of Z-stacks that were

acquired using a Leica SP8 inverted confocal microscope with 10x HC PL APO CS, 20x HC PL APO IMM/CORR CS2 and 63x HC PL APO Oil CS2 objectives and Leica LAS-X software.

Statistics. GraphPad Prism was used for graphic representation and statistical analysis of data. A two-tailed unpaired Student's t-test was used to compare between two means, assuming equal variance. Differences were considered statistically significant when $p<0.05$. The experiments were not randomized. No blinding was done for the analysis and quantification studies.

Data availability. All relevant data are available from the corresponding author upon request. The mass spectrometry proteomics data have been deposited to the ProteomeXchange Consortium [22] via the PRIDE [23] partner repository with the dataset identifier PXD020216.

Results

FXII is enriched and activated in lung tissue from COVID-19 patients.

To comprehensively screen for pathways that contribute to thrombo-inflammation in COVID-19 patients that succumbed to the disease, we performed differential proteomic analysis of postmortem lung tissue from COVID-19 patients (n=3) and control patients with COVID-19-independent lung pathologies (n=3) (Figure 1 and clinical characteristics of patients in Supplemental figure 1A). Gene Ontology (GO) analysis identified enrichment of pathways related to (i) classical complement activation (green), (ii) activation of proangiogenic pathways (red) as well as (iii) platelet degranulation (magenta) and (iv) neutrophil activation and degranulation (blue) in lungs of COVID-19 patients (Figure 1B). Consistently, immunofluorescence staining of COVID-19 lung vibratome sections that allow for three-dimensional visualization of the tissue architecture showed adherent degranulated platelets at the wall of microvessels using a CD62P antibody (Supplemental figure 2). These findings are consistent with described platelet activation in COVID-19 [24,25].

To identify key players of COVID-19-associated thrombo-inflammation in an unbiased approach, we performed protein association network analysis (https://string-db.org) of the proteomic data obtained from COVID-19 lung tissue (Figure 1C). We found peptides of the FXII sequence enriched in lungs from patient COVID-19-1 and patient COVID-19-3 (Figure 1C). In line with previous studies [3] and indicative of a procoagulant state, proteomic analysis revealed an increase in fibrinogen protein complexes (fibrinogen alpha (log2fold change 1.73), beta (1.5), gamma chains (1.64)) in COVID-19 lungs (data not shown). Immunofluorescence analysis of COVID-19 lung vibratome sections using antibodies against fibrin and Collagen I showed dense fibrin sheet depositions at the alveolar walls (Figure 1D, arrows).

FXII is converted to FXIIa by limited proteolysis of a single peptide bond. While proteomics approach detected FXII specific peptides, the method is insensitive to discriminate whether the FXII zymogen form or the active protease FXIIa is enriched in lung tissues of COVID-19 patients. To directly test if FXII is activated in COVID-19 lungs, we performed immunostaining of vibratome sections from COVID-19 lungs using antibodies against FXIIa (3F7) [26] and Collagen I (Figure 2). 3F7 specifically binds to FXIIa and has no detectable cross-reactivity with the FXII zymogen form[27]. 3F7 immunostaining demonstrated that FXII is activated in lung parenchyma, within the pulmonary vessel walls and in fibrin-rich alveolar spaces of COVID-19 lung tissue (Figure 2). In contrast, no increased FXIIa signal was detectable in lung tissue from patients that died from Acute Respiratory Distress Syndrome (ARDS) (Figure 2). These results show that FXIIa is enriched in COVID-19 lungs and therefore likely contributes to pulmonary thrombo-inflammatory processes.

NETs activate FXII in COVID-19 lungs.

Next, we sought to analyse the mechanism by which FXII is activated in COVID-19. NETs have been shown to initiate FXIIa formation *ex vivo* [12]. Furthermore, increased NETs formation has been shown in serum samples and lung tissue from COVID-19 patients [17-19]. In line with these previous findings, immunofluorescence staining of vibratome sections with antibodies against the NETs biomarker neutrophil elastase (NE) and chromatin visualized degranulated neutrophils releasing elongated chromatin-positive NETs into the lung parenchyma and the alveolar spaces (Figure 3A). Consistent with the immunofluorescence, NETs-specific markers such as circulating extracellular DNA and myeloperoxidase were increased in plasma samples from COVID-19 patients ($n = 24$) over healthy control donors ($n = 5$) (Supplemental figure 1B, 3A+B). NETs biomarkers correlated with lactate dehydrogenase (cell destruction biomarker) ($r = 0.8252$; $p < 0.0001$), total leukocytes ($r = 0.7978$; $p = 0.0001$) and C-reactive protein (marker of inflammation) ($r = 0.4855$; $p = 0.0189$) (Supplemental figure 3C).

To test if NETs can provide a scaffold to induce FXII contact activation in COVID-19 lungs, we performed high resolution immunostaining of lung vibratome sections from COVID-19 lungs using antibodies against FXIIa (3F7) and the NETs component citrullinated histone 3 (Figure 3B). FXIIa co-localized with NETs, indicating that NETs induced FXII activation in COVID-19 lung tissue.

Defective NETs clearance underlies sustained FXII activation in COVID-19 lungs.

As NETs are abundant in the circulation, lung parenchyma and alveolar spaces of COVID-19 patients, we next sought to identify the underlying mechanism of NETs accumulation. Two

independent experimental approaches analyzed for DNase activity in plasma samples from COVID-19 patients. Both assays showed that DNase activity was reduced in plasma samples from COVID-19 patients compared to levels in heathy donors (Figure 4A+B). Furthermore, defective DNase activity was corroborated in a third NETs degradation assay where *in vitro* generated NETs were incubated with plasma either from COVID-19 patients or healthy donors (Figure 4C). Healthy donor plasma or recombinant human DNase I (Pulmozyme, data not shown) completely degraded NETs within 3h. In contrast, COVID-19 plasma was inactive to degrade NETs (Figure 4C). We conclude that excessive NET accumulation in COVID-19 results from increased generation and impaired degradation of NETs.

To evaluate a potential therapeutic approach for interference with the NETs/FXIIa axis, we tested if accelerated NETs clearance through DNase I addition impacts on FXII activation. To that end, healthy human neutrophils were activated to produce NETs (10nM, phorbol 12-myristate 13-acetate, PMA) and formation of FXIIa was analyzed by a chromogenic assay (Figure 4D). Vice versa, degradation of NETs following addition of DNase I (Pulmozyme) reduced FXIIa formation by about half (51%). The FXII inhibitor rHA-infestin-4, on the other hand, completely suppressed FXIIa signal (Figure 4C). Taken together, we show that defective NETs clearance underlies sustained FXII activation in COVID-19-associated pulmonary thrombo-inflammation. Besides targeting FXIIa, these data suggest therapeutically targeting of the FXII contact activator NETs in COVID-19.

Discussion

Our study uncovers a role of NETs-induced activation of FXII for COVID-19-associated thrombo-inflammation. Two types of thrombotic complications occur in COVID-19 patients: DVT with pulmonary embolism can be frequently observed, especially in patients receiving intensive care [28]. On the other hand, COVID-19 patients also have a nine times higher prevalence of alveolar-capillary microthrombi compared to patients with influenza [29]. There is a high incidence of venous thromboembolic events in severe COVID-19 cases, despite prophylactic anticoagulation [30,31]. Even after hospital discharge of COVID-19 patients, thrombotic events can be frequently observed, demonstrating the importance of extended thromboprophylaxis [32]. Therefore, additional treatment targeting novel thrombo-inflammatory mediators could help to mitigate COVID-19-induced thrombotic complications.

Strikingly, in-hospital mortality of patients on mechanical ventilation was reduced by 50% upon receiving treatment-dose anticoagulation and prophylactic treatment plan including a higher anticoagulation regiment could ameliorate the disease severity in COVID-19 cases [33]. Improved survival seems to be attributed to efficient prophylaxis of pulmonary microthrombi. Since more potent anticoagulation is often associated with an increased bleeding risk, alternative approaches, which target coagulation but spare hemostasis, are needed.

COVID-19 infection has been shown to cause inflammation of endothelial cells (ECs) (endotheliitis) [29]. Proteomic analysis of COVID-19 lungs showed enrichment of pathways associated with angiogenesis and vascular development suggesting induction of blood vessel growth in COVID-19 lungs (Figure 1B). In line with this, intussusceptive angiogenesis was increased in lungs of COVID-19 patients compared to patients with influenza infection [29]. Furthermore, we found upregulation of complement system proteins in COVID-19 lungs. This is in line with previous publications that suggested that complement and NETs contribute to COVID-19 immuno-thrombosis [34,35].

We found FXII to be enriched in COVID-19 lung tissue but not in lung tissue from other lung diseases. The 3F7 antibody, which specifically detects FXIIa [26], showed enriched FXII is at least activated in lung parenchyma, within the pulmonary vessel walls and in fibrin-rich alveolar spaces of COVID-19 lungs. Colocalization of NETs and FXIIa in COVID-19 lung immunostaining indicates that NETs provide a platform for FXII contact activation in COVID-19 and possibly other NETs-driven disease states. The high plasma concentration of FXII (450 nM) together with increased endothelial barrier permeability (that leads to pulmonary edema in COVID-19 patients), suggests that leakage of FXII into subendothelial tissues might take place. In previous studies, we showed that neutrophils express a pool of FXII that is functionally

distinct from hepatic-derived FXII and contributes to NETs formation [36], suggesting that enriched FXII might also originate from infiltrated neutrophils in COVID-19 lungs.

In line with published studies [17-19], we showed excessive NETs accumulation in COVID-19 plasma and lung tissue. Defective NETs degradation amplifies NETs cytotoxic activities and under physiologic conditions host DNases critically regulate NETs turnover [20]. Indeed, elevated NETs accumulation has been associated with reduced DNase activity in thrombotic microangiopathies and sepsis [37]. Although, the initial trigger of NETs formation during COVID-19 is not properly understood, we observed a reduced DNase activity in COVID-19 patient plasma, which was accompanied by an impaired capacity to digest *in vitro* generated NETs from healthy neutrophils. Furthermore, improved NETs clearance through exogenous DNase I reduced FXII activation *in vitro*, suggesting that COVID-19 patients could benefit from DNase I treatment. Currently, there are nine interventional clinical trials ongoing that investigate the safety and efficacy of DNases, including the recombinant human DNase I (Pulmozyme) in COVID-19 patients (ClinicalTrials.gov identifiers: NCT04355364, NCT04402970, NCT04445285, NCT04432987, NCT04359654, NCT04402944, NCT04524962, NCT04541979 and NCT04409925).

Besides its well-known selective role in thrombosis[13], FXII drives production of the inflammatory mediator bradykinin. The activity of bradykinin is controlled through degradation of the peptide hormone by several broad-spectrum cell-surface associated peptidases, including angiotensin-converting enzyme (ACE), dipeptidyl peptidase 4 (DPP4) and aminopeptidase P [38]. Furthermore, its derivative des-Arg^9-bradykinin is a target for degradation by ACE-2, the receptor that SARS-CoV-2 uses to enter cells [39]. The exact role of ACE-2 remains to be shown as a recent systems biology study surprisingly showed that ACE-2 levels, which were suspected to be downregulated as a result of virus entry, were elevated in plasma samples of male COVID-19 patients [40]. On the other hand, plasma levels of DPP4 (an uptake receptor for coronaviruses, but not for SARS-CoV-2) levels are reduced [40], suggesting dysregulated bradykinin signaling in COVID-19. Target bradykinin production or signaling appears to attenuate pulmonary edema in COVID-19 patients [41,42]. Our study provides additional evidence for a role of the kallikrein kinin-system in COVID-19; carboxypeptidase N (CPN1) was exclusively found in COVID-19 lung tissue (Figure 1C), which would result in accelerated conversion of bradykinin to des-Arg^9-bradykinin. Finally, we found reduced levels of aminopeptidase N (ANPEP) in lungs of COVID-19 patients (Figure 1A). This enzyme (another receptor for coronaviridae, https://www.ncbi.nlm.nih.gov/gene/290) is expressed by numerous cell types, including inflammatory cells [43]. ANPEP plays a role in the activation of chemokines and trimming of antigens prior to their presentation. Interestingly, the activity of

this enzyme is competitively blocked by bradykinin (and therapeutic analogs [44,45]). This suggests that besides its direct proinflammatory roles, increased bradykinin levels may indirectly contribute to inflammation by repressing ANPEP activity in COVID-19 patients.

Activated FXII drives coagulation in various vascular beds [46] and the formation of bradykinin suggesting that activated FXII itself is an attractive drug target for interference with thrombo-inflammation. Together with CSL Behring, we have previously demonstrated that targeting FXIIa with the neutralizing antibody 3F7 provides thrombo-protection and impedes bradykinin production in a preclinical setting [27]. Recently, CSL Behring has initiated a clinical trial to test efficacy of the FXIIa neutralizing antibody CSL312 (Garadacimab, a successor molecule of 3F7) in COVID-19 patients (ClinicalTrials.gov Identifier: NCT04409509).

In conclusion, we uncovered a role of defective NETs clearance in sustained FXII contact activation in COVID-19-associated pulmonary thrombo-inflammation. Our data put the NETs/FXII axis in a central position in COVID-19-induced lung disease and suggest novel therapeutic strategies that target both, NETs and FXIIa, for safe interference with COVID-19-induced thrombo-inflammation and beyond.

Author contributions

H.E., C.R., C.D. and C.K. performed plasma experiments, M.F., H.E., JP.S., C.K. and D.S. performed lung tissue experiments. E.G., S.K., G.P., R.M., F.L. EX.S. and C.M. conceived and discussed data. M.H. and K.Pü. provided resources. K.Pa. and H.S. provided essential tools. H.E., C.R., C.D., T.R. and M.F. wrote the manuscript. M.F. conceived and directed the study; all authors discussed the results and commented on the manuscript.

Acknowledgements

We thank the UKE Microscopy Imaging Facility for technical microscopy support. This study was supported by the European Union's Horizon 2020 Research and Innovation Programme under the Marie Skłodowska-Curie Grant Agreement No. 840189, the Werner Otto Medical Foundation Hamburg (8/95) and German Research Foundation (DFG) grant FR 4239/1-1 (to M.F.) and grants A11/SFB877, B08/SFB841 and P06/KFO306 of the DFG (to T.R.).

Disclosures

The authors declare no competing financial interests.

References

1. Huang C, Wang Y, Li X, Ren L, Zhao J, Hu Y, et al. Clinical features of patients infected with 2019 novel coronavirus in Wuhan, China. *Lancet.* 2020;395(10223):497-506.
2. Pedersen SF, Ho Y-C. SARS-CoV-2: a storm is raging. *The Journal of Clinical Investigation.* 2020;130(5):2202-2205.
3. Wichmann D, Sperhake JP, Lutgehetmann M, Steurer S, Edler C, Heinemann A, et al. Autopsy Findings and Venous Thromboembolism in Patients With COVID-19. *Ann Intern Med.* 2020.
4. Rapkiewicz Amy V. XM, Steven E. Carsons, Stefania Pittaluga, David E. Kleiner, Jeffrey S. Berger, Sarun Thomas, Nicole M. Adler, David M. Charytan, Billel Gasmi,, Judith S. Hochman HRR. Megakaryocytes and platelet-fibrin thrombi characterize multi-organ thrombosis at autopsy in COVID-19: A case series. *EClinicalMedicine.* 2020.
5. Edler C, Schroder AS, Aepfelbacher M, Fitzek A, Heinemann A, Heinrich F, et al. Dying with SARS-CoV-2 infection-an autopsy study of the first consecutive 80 cases in Hamburg, Germany. *Int J Legal Med.* 2020;134(4):1275-1284.
6. Fox SE, Akmatbekov A, Harbert JL, Li G, Quincy Brown J, Vander Heide RS. Pulmonary and cardiac pathology in African American patients with COVID-19: an autopsy series from New Orleans. *Lancet Respir Med.* 2020.
7. Barnes BJ, Adrover JM, Baxter-Stoltzfus A, Borczuk A, Cools-Lartigue J, Crawford JM, et al. Targeting potential drivers of COVID-19: Neutrophil extracellular traps. *J Exp Med.* 2020;217(6).
8. McDonald B, Pittman K, Menezes GB, Hirota SA, Slaba I, Waterhouse CC, et al. Intravascular danger signals guide neutrophils to sites of sterile inflammation. *Science.* 2010;330(6002):362-366.
9. Page AR, Good RA. A clinical and experimental study of the function of neutrophils in the inflammatory response. *Am J Pathol.* 1958;34(4):645-669.
10. Fuchs TA, Brill A, Duerschmied D, Schatzberg D, Monestier M, Myers DD, Jr., et al. Extracellular DNA traps promote thrombosis. *Proc Natl Acad Sci U S A.* 2010;107(36):15880-15885.
11. Massberg S, Grahl L, von Bruehl ML, Manukyan D, Pfeiler S, Goosmann C, et al. Reciprocal coupling of coagulation and innate immunity via neutrophil serine proteases. *Nat Med.* 2010;16(8):887-896.
12. von Bruhl ML, Stark K, Steinhart A, Chandraratne S, Konrad I, Lorenz M, et al. Monocytes, neutrophils, and platelets cooperate to initiate and propagate venous thrombosis in mice in vivo. *J Exp Med.* 2012;209(4):819-835.
13. Renné T, Stavrou EX. Roles of Factor XII in Innate Immunity. *Frontiers in Immunology.* 2019;10(2011).
14. Gould TJ, Vu TT, Swystun LL, Dwivedi DJ, Mai SHC, Weitz JI, et al. Neutrophil Extracellular Traps Promote Thrombin Generation Through Platelet-Dependent and Platelet-Independent Mechanisms. *Arteriosclerosis, Thrombosis, and Vascular Biology.* 2014;34(9):1977-1984.
15. Jimenez-Alcazar M, Rangaswamy C, Panda R, Bitterling J, Simsek YJ, Long AT, et al. Host DNases prevent vascular occlusion by neutrophil extracellular traps. *Science.* 2017;358(6367):1202-1206.
16. Grabcanovic-Musija F, Obermayer A, Stoiber W, Krautgartner WD, Steinbacher P, Winterberg N, et al. Neutrophil extracellular trap (NET) formation characterises stable and exacerbated COPD and correlates with airflow limitation. *Respir Res.* 2015;16:59.
17. Middleton EA, He X-Y, Denorme F, Campbell RA, Ng D, Salvatore SP, et al. Neutrophil Extracellular Traps (NETs) Contribute to Immunothrombosis in COVID-19 Acute Respiratory Distress Syndrome. *Blood.* 2020.
18. Zuo Y, Yalavarthi S, Shi H, Gockman K, Zuo M, Madison JA, et al. Neutrophil extracellular traps in COVID-19. *JCI Insight.* 2020;5(11).

19. Veras FP, Pontelli M, Silva C, Toller-Kawahisa J, de Lima M, Nascimento D, et al. SARS-CoV-2 triggered neutrophil extracellular traps (NETs) mediate COVID-19 pathology. *medRxiv.* 2020:2020.2006.2008.20125823.
20. Jiménez-Alcázar M, Rangaswamy C, Panda R, Bitterling J, Simsek YJ, Long AT, et al. Host DNases prevent vascular occlusion by neutrophil extracellular traps. *Science.* 2017;358(6367):1202.
21. Brinkmann V, Reichard U, Goosmann C, Fauler B, Uhlemann Y, Weiss DS, et al. Neutrophil extracellular traps kill bacteria. *Science.* 2004;303(5663):1532-1535.
22. Deutsch EW, Bandeira N, Sharma V, Perez-Riverol Y, Carver JJ, Kundu DJ, et al. The ProteomeXchange consortium in 2020: enabling 'big data' approaches in proteomics. *Nucleic Acids Res.* 2020;48(D1):D1145-d1152.
23. Perez-Riverol Y, Csordas A, Bai J, Bernal-Llinares M, Hewapathirana S, Kundu DJ, et al. The PRIDE database and related tools and resources in 2019: improving support for quantification data. *Nucleic Acids Res.* 2019;47(D1):D442-d450.
24. Manne BK, Denorme F, Middleton EA, Portier I, Rowley JW, Stubben C, et al. Platelet gene expression and function in patients with COVID-19. *Blood.* 2020;136(11):1317-1329.
25. Hottz ED, Azevedo-Quintanilha IG, Palhinha L, Teixeira L, Barreto EA, Pao CRR, et al. Platelet activation and platelet-monocyte aggregate formation trigger tissue factor expression in patients with severe COVID-19. *Blood.* 2020;136(11):1330-1341.
26. Worm M, Kohler EC, Panda R, Long A, Butler LM, Stavrou EX, et al. The factor XIIa blocking antibody 3F7: a safe anticoagulant with anti-inflammatory activities. *Ann Transl Med.* 2015;3(17):247.
27. Larsson M, Rayzman V, Nolte MW, Nickel KF, Björkqvist J, Jämsä A, et al. A factor XIIa inhibitory antibody provides thromboprotection in extracorporeal circulation without increasing bleeding risk. *Sci Transl Med.* 2014;6(222):222ra217.
28. Middeldorp S, Coppens M, van Haaps TF, Foppen M, Vlaar AP, Müller MCA, et al. Incidence of venous thromboembolism in hospitalized patients with COVID-19. *J Thromb Haemost.* 2020.
29. Ackermann M, Verleden SE, Kuehnel M, Haverich A, Welte T, Laenger F, et al. Pulmonary Vascular Endothelialitis, Thrombosis, and Angiogenesis in Covid-19. *New England Journal of Medicine.* 2020.
30. Llitjos JF, Leclerc M, Chochois C, Monsallier JM, Ramakers M, Auvray M, et al. High incidence of venous thromboembolic events in anticoagulated severe COVID-19 patients. *J Thromb Haemost.* 2020;18(7):1743-1746.
31. Langer F, Kluge S, Klamroth R, Oldenburg J. Coagulopathy in COVID-19 and Its Implication for Safe and Efficacious Thromboprophylaxis. *Hamostaseologie.* 2020.
32. Patell R, Bogue T, Koshy A, Bindal P, Merrill M, Aird WC, et al. Postdischarge thrombosis and hemorrhage in patients with COVID-19. *Blood.* 2020;136(11):1342-1346.
33. Paranjpe I, Fuster V, Lala A, Russak AJ, Glicksberg BS, Levin MA, et al. Association of Treatment Dose Anticoagulation With In-Hospital Survival Among Hospitalized Patients With COVID-19. *Journal of the American College of Cardiology.* 2020;76(1):122.
34. Magro C, Mulvey JJ, Berlin D, Nuovo G, Salvatore S, Harp J, et al. Complement associated microvascular injury and thrombosis in the pathogenesis of severe COVID-19 infection: A report of five cases. *Translational Research.* 2020;220:1-13.
35. Skendros P, Mitsios A, Chrysanthopoulou A, Mastellos DC, Metallidis S, Rafailidis P, et al. Complement and tissue factor-enriched neutrophil extracellular traps are key drivers in COVID-19 immunothrombosis. *medRxiv.* 2020:2020.2006.2015.20131029.
36. Stavrou EX, Fang C, Bane KL, Long AT, Naudin C, Kucukal E, et al. Factor XII and uPAR upregulate neutrophil functions to influence wound healing. *The Journal of Clinical Investigation.* 2018;128(3):944-959.
37. Fuchs TA, Kremer Hovinga JA, Schatzberg D, Wagner DD, Lämmle B. Circulating DNA and myeloperoxidase indicate disease activity in patients with thrombotic microangiopathies. *Blood.* 2012;120(6):1157-1164.

38. de Maat S, de Mast Q, Danser AHJ, van de Veerdonk FL, Maas C. Impaired Breakdown of Bradykinin and Its Metabolites as a Possible Cause for Pulmonary Edema in COVID-19 Infection. *Semin Thromb Hemost.* 2020.
39. Zhou P, Yang XL, Wang XG, Hu B, Zhang L, Zhang W, et al. A pneumonia outbreak associated with a new coronavirus of probable bat origin. *Nature.* 2020;579(7798):270-273.
40. van de Veerdonk FL, Janssen NAF, Grondman I, de Nooijer AH, Koeken VACM, Matzaraki V, et al. A systems approach to inflammation identifies therapeutic targets in SARS-CoV-2 infection. *medRxiv.* 2020:2020.2005.2023.20110916.
41. van de Veerdonk FL, Netea MG, van Deuren M, van der Meer JWM, de Mast Q, Brüggemann RJ, et al. Kallikrein-kinin blockade in patients with COVID-19 to prevent acute respiratory distress syndrome. *eLife.* 2020;9:e57555.
42. van de Veerdonk FL, Kouijzer IJE, de Nooijer AH, van der Hoeven HG, Maas C, Netea MG, et al. Outcomes Associated With Use of a Kinin B2 Receptor Antagonist Among Patients With COVID-19. *JAMA Netw Open.* 2020;3(8):e2017708-e2017708.
43. Luan Y, Xu W. The structure and main functions of aminopeptidase N. *Curr Med Chem.* 2007;14(6):639-647.
44. Xu Y, Wellner D, Scheinberg DA. Substance P and bradykinin are natural inhibitors of CD13/aminopeptidase N. *Biochem Biophys Res Commun.* 1995;208(2):664-674.
45. Bawolak MT, Fortin JP, Vogel LK, Adam A, Marceau F. The bradykinin B2 receptor antagonist icatibant (Hoe 140) blocks aminopeptidase N at micromolar concentrations: off-target alterations of signaling mediated by the bradykinin B1 and angiotensin receptors. *Eur J Pharmacol.* 2006;551(1-3):108-111.
46. Maas C, Renné T. Coagulation factor XII in thrombosis and inflammation. *Blood.* 2018;131(17):1903-1909.

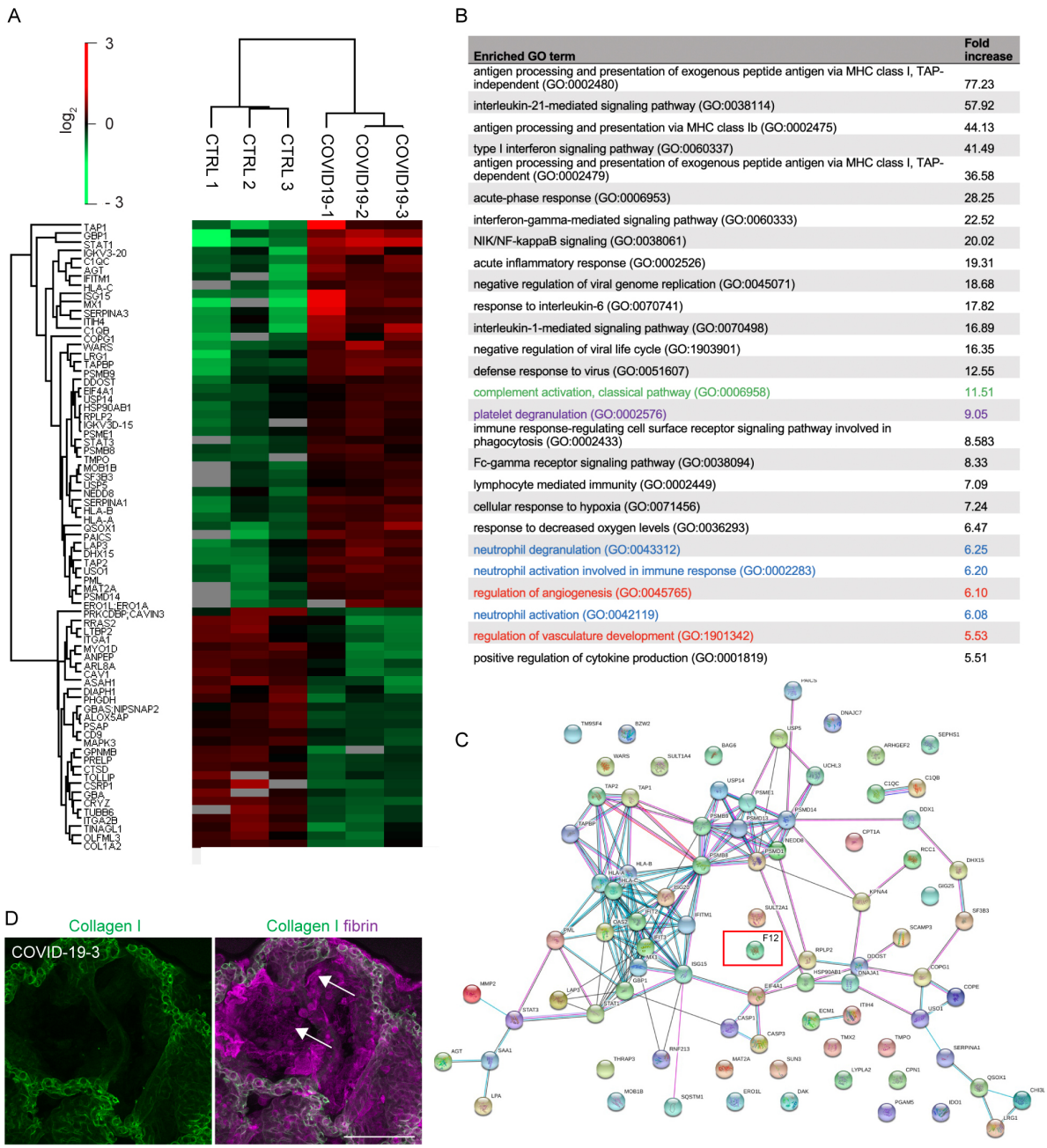

Enriched GO term	Fold increase
antigen processing and presentation of exogenous peptide antigen via MHC class I, TAP-independent (GO:0002480)	77.23
interleukin-21-mediated signaling pathway (GO:0038114)	57.92
antigen processing and presentation via MHC class Ib (GO:0002475)	44.13
type I interferon signaling pathway (GO:0060337)	41.49
antigen processing and presentation of exogenous peptide antigen via MHC class I, TAP-dependent (GO:0002479)	36.58
acute-phase response (GO:0006953)	28.25
interferon-gamma-mediated signaling pathway (GO:0060333)	22.52
NIK/NF-kappaB signaling (GO:0038061)	20.02
acute inflammatory response (GO:0002526)	19.31
negative regulation of viral genome replication (GO:0045071)	18.68
response to interleukin-6 (GO:0070741)	17.82
interleukin-1-mediated signaling pathway (GO:0070498)	16.89
negative regulation of viral life cycle (GO:1903901)	16.35
defense response to virus (GO:0051607)	12.55
complement activation, classical pathway (GO:0006958)	11.51
platelet degranulation (GO:0002576)	9.05
immune response-regulating cell surface receptor signaling pathway involved in phagocytosis (GO:0002433)	8.583
Fc-gamma receptor signaling pathway (GO:0038094)	8.33
lymphocyte mediated immunity (GO:0002449)	7.09
cellular response to hypoxia (GO:0071456)	7.24
response to decreased oxygen levels (GO:0036293)	6.47
neutrophil degranulation (GO:0043312)	6.25
neutrophil activation involved in immune response (GO:0002283)	6.20
regulation of angiogenesis (GO:0045765)	6.10
neutrophil activation (GO:0042119)	6.08
regulation of vasculature development (GO:1901342)	5.53
positive regulation of cytokine production (GO:0001819)	5.51

Figure 1. Proteomic analysis reveals enrichment of FXII and pathways involved in platelet, complement and neutrophil activation in lung tissue from COVID-19 patients. (A) Heatmap of differentially regulated proteins in the lung tissue of patients with COVID-19 and COVID-19-independent lung pathologies (CTRL) (n = 3 each). (B) Selected Gene Ontology (GO) terms of enriched proteins in COVID-19 lungs highlighting pathways involved in platelet (magenta), complement (green) and neutrophil activation (blue) and angiogenesis (red). (C) Protein association network analysis (https://string-db.org) of enriched proteins in COVID-19 lungs. (D) Representative immunofluorescence of lung vibratome sections using antibodies against Collagen I (green) and fibrin (magenta) shows large fibrin depositions lining the alveolar space of FXII-enriched COVID-19 lungs (white arrows). Scale bar: 100 µm.

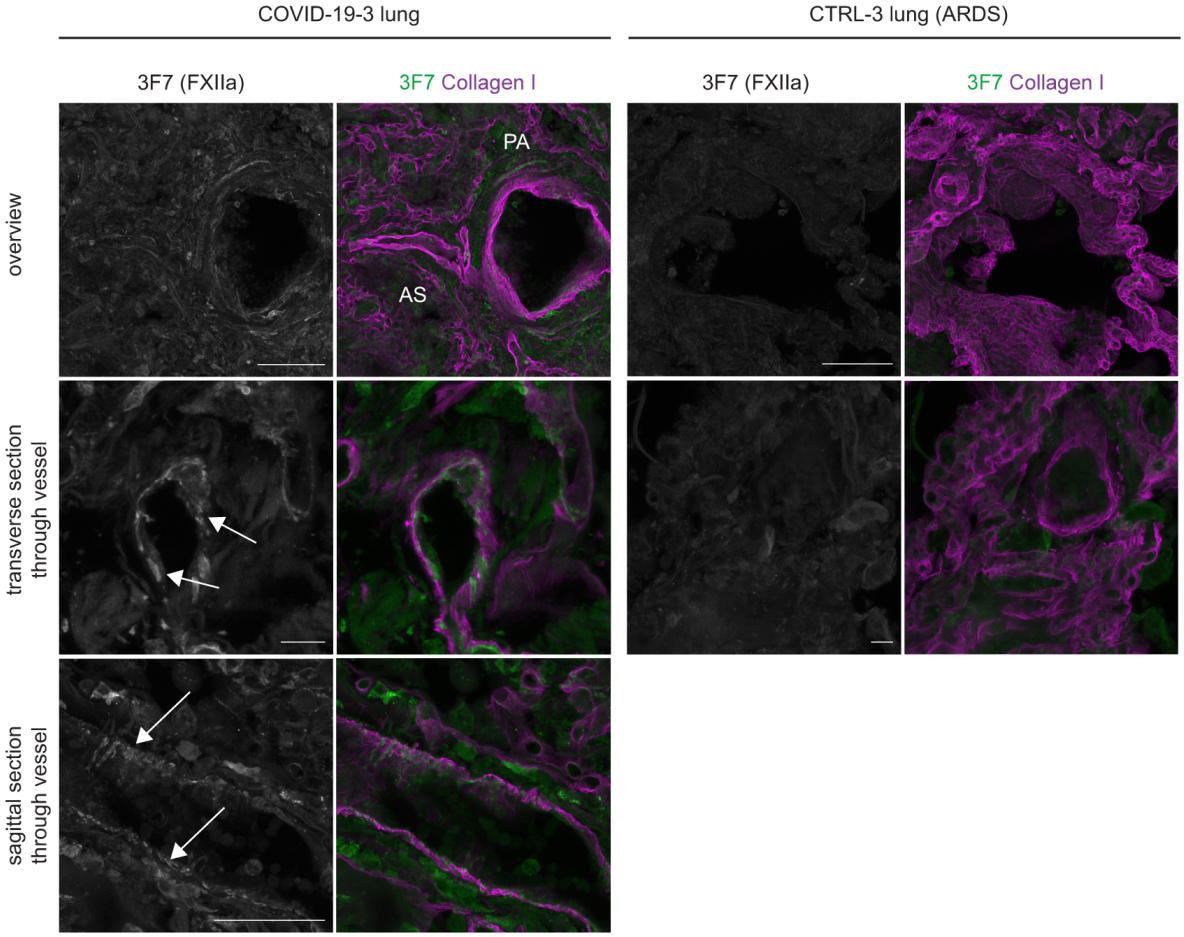

Figure 2. FXII is activated in COVID-19 lungs.

Representative immunofluorescence of vibratome sections from FXII-enriched COVID-19 and Acute Respiratory Distress Syndrome (ARDS) control lungs using antibodies against FXIIa (3F7, green or grey in single channel images) and Collagen I (magenta). Alveolar space (AS), parenchyma (PA). Scale bar: 100 µm top/10 µm middle/50 µm bottom panel.

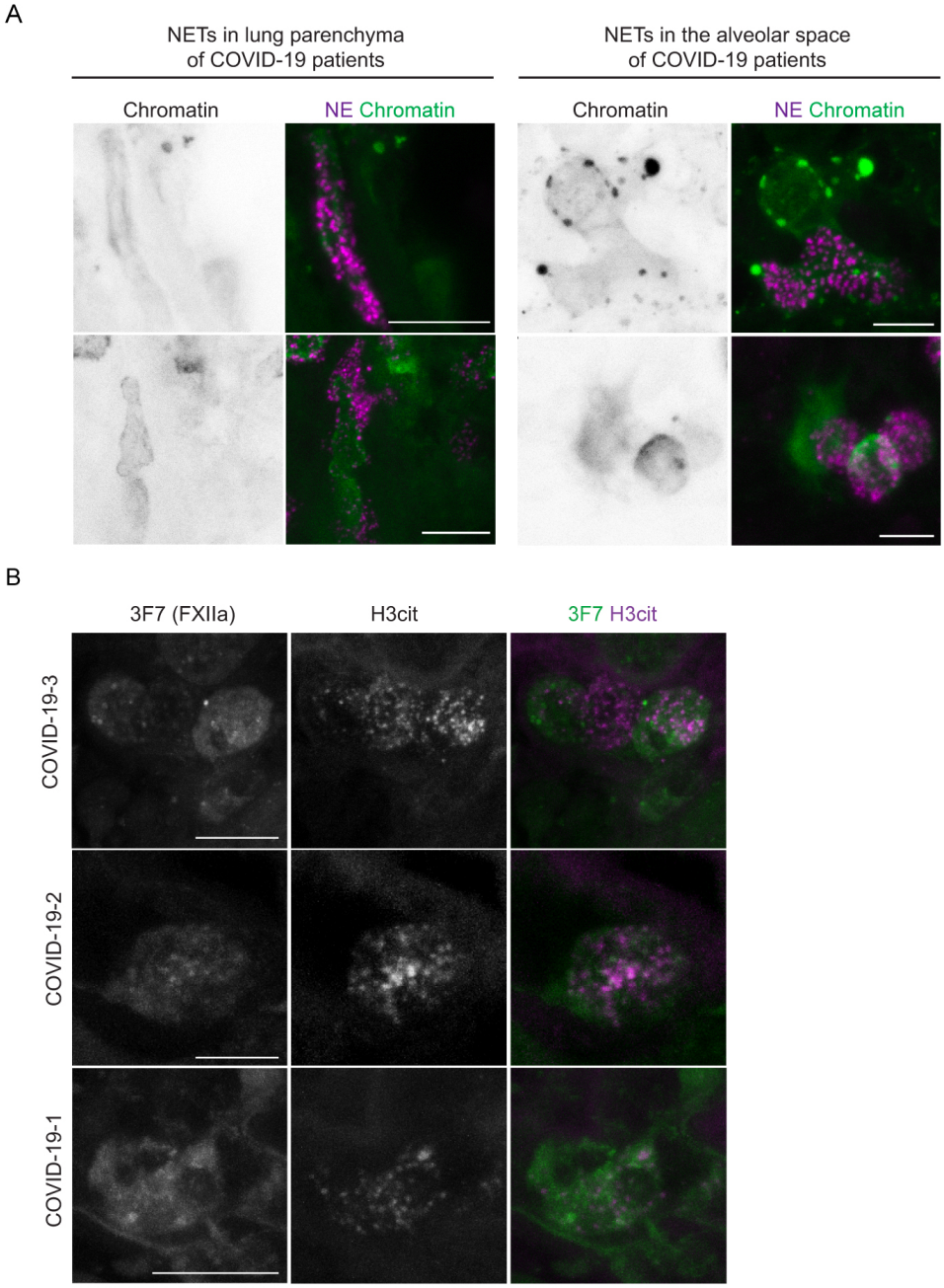

Figure 3. NETs and FXIIa colocalize in COVID-19 lungs.

(A) High magnification immunofluorescence images of NETs in the lung parenchyma and the alveolar spaces using antibodies against NE (magenta) and chromatin (green or grey in single channel images). (B) Representative immunofluorescence of vibratome sections COVID-19 lungs using antibodies against activated FXII (3F7, green or grey in single channel images) and histone 3 (H3cit) (magenta or grey in single channel images. Scale bar: 10 µm (A, B).

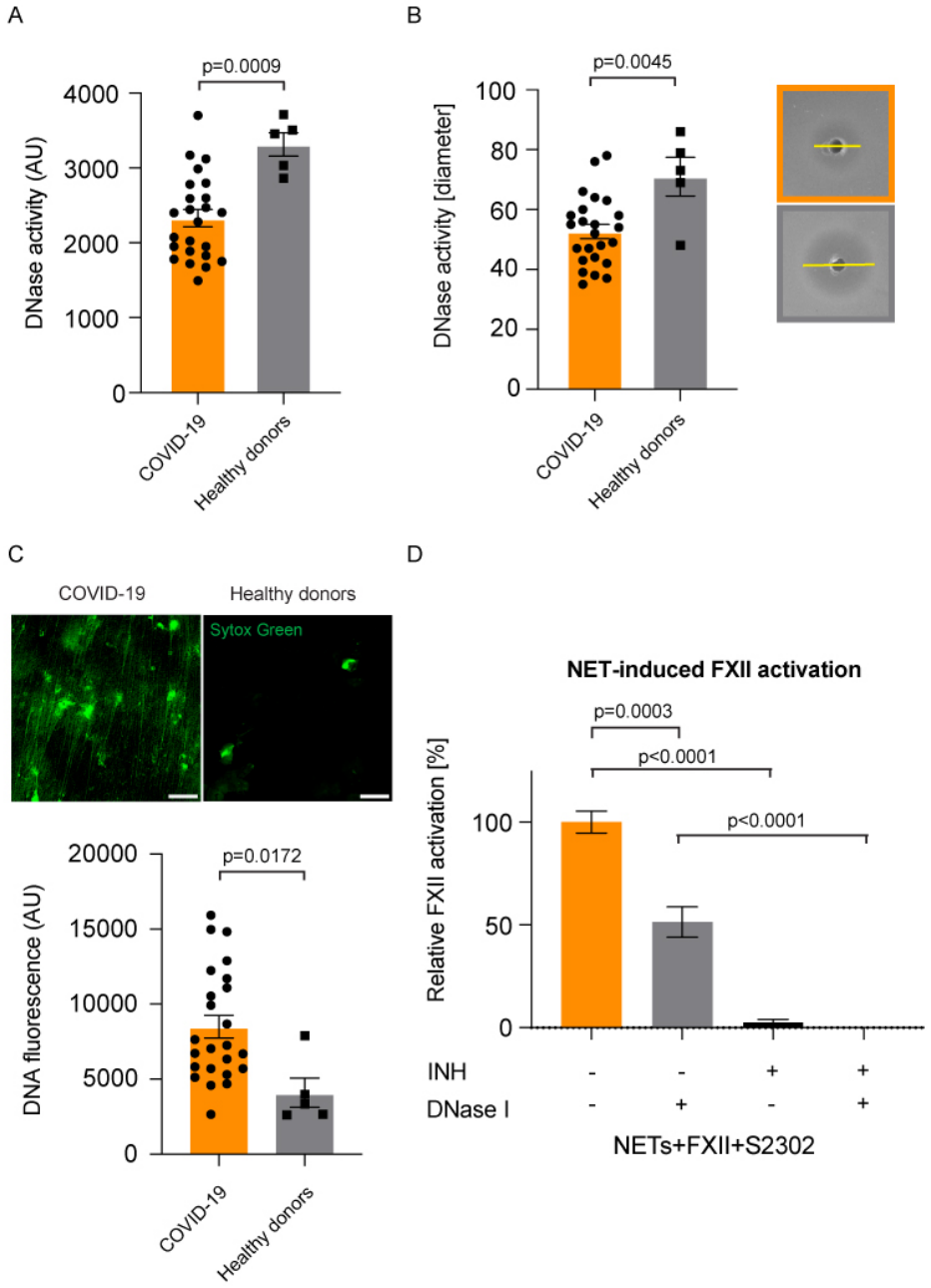

Figure 4: Delayed NETs clearance due to defective DNase activity in COVID-19.

(A) DNase activity measured in plasma samples from COVID-19 patients (n = 24) or healthy donors (n = 5) using the DNase Alert QC System. Data represent mean ± s.e.m., p-value, two-tailed unpaired Student's t-test. (B) DNase activity measured in plasma samples from COVID-19 patients (n = 24) or healthy donors (n = 5) using the SRED assay. Representative pictures are shown for COVID-19 (orange box) and healthy donors (grey box). Data represent mean ± s.e.m., p-value, two-tailed unpaired Student's t-test. (C) NET degradation capacity of COVID-19 plasma. DNA fluorescence was quantified from COVID-19 plasma (n = 24) and healthy donor plasma (n = 5). Data represent mean ± s.e.m., p-value, two-tailed unpaired Student's t-test. Representative immunofluorescence images of *in vitro* generated NETs upon incubation with healthy donor or COVID-19 plasma are shown. (D) Activation of purified FXII by NETs

was measured by conversion of the chromogenic substrate D-Pro-Phe-Arg-p-nitroanilide (S-2302) at an absorption of λ=405 nm. S-2302 was added either in the presence or absence of the FXIIa inhibitor rHA-infestin-4 (INH) or DNase I (Pulmozyme). Data represent mean ± s.e.m., p-value, two-tailed unpaired Student's t-test (n = 6 replicates per time point from two independent experiments). Arbitrary units (AU), Scale bar: 25 μm (C).